RZ 2957 (# 93003) 09/22/97
Chemistry 08 pages

# Research Report

## Interaction of Alzheimer's Disease $\beta$–amyloid Peptide with Aluminum in Water Solution: A Classical Molecular Dynamics Study

Paolo Carloni

IBM Research Division
Zurich Research Laboratory
8803 Rüschlikon
Switzerland

Present address: Laboratory of Inorganic and Bioinorganic Chemistry
Department of Chemistry
University of Florence
Via G. Capponi 7
50100 Firenze
Italy

# Interaction of Alzheimer's Disease $\beta$–amyloid Peptide with Aluminum in Water Solution: A Classical Molecular Dynamics Study

Paolo Carloni[1,2]

*IBM Research Division, Zurich Research Laboratory, 8803 Rüschlikon, Switzerland*

## Abstract

The structure and dynamics of the Alzheimer's disease $\beta$–amyloid (1–40) peptide and its adducts with aluminum in aqueous solution are investigated using classical molecular dynamics simulations. The calculations indicate (i) that the peptide is stable in water solution and (ii) that $Al^{3+}$ does not destabilize the secondary structure of the peptide. The formation of peptide–peptide cross links may be the cause of the Al-promoted peptide aggregation found experimentally.

[1]Telephone: +41-1-724-8490; Fax: +41-1-724-8952; e-mail: cap@zurich.ibm.com

[2]Present address: Laboratory of Inorganic and Bioinorganic Chemistry, Department of Chemistry, University of Florence, Via G. Capponi 7, 50100 Firenze, Italy

# Introduction

Aluminum is a suspected risk factor in the pathogenesis of Alzheimer's disease (AD) (Crapper *et al.*, 1973; Perl & Brody, 1980; Exley *et al.*, 1993; Corain *et al.*, 1996; Good & Perl, 1993; Newman, 1992; Kawahara *et al.*, 1994; Fasman *et al.*, 1995; Wisniewski & Wen, 1992). Aluminum has been found to accumulate in the AD-specific cerebral lesions, intraneuronal neurofibrillary tangles, and extracellular amyloid plaques, although evidence of its presence is apparently controversial (Landsberg *et al.*, 1992; Good & Perl, 1993).

Attention has been focused on the interaction between Al(III) and the major component of the amyloid plaques, the 39–42-residue Alzheimer's $\beta$-amyloid peptide (A$\beta$P). Al(III) is found to (i) substantially enhance the peptide aggregation in fluorinated alcohol (Exley *et al.*, 1993; Fasman *et al.*, 1995) and (ii) induce the formation of amyloid plaques in vitro (Kawahara *et al.*, 1994), which is believed to be a crucial process in the pathogenesis of AD (Selkoe, 1997).

Clearly, understanding the mechanism of the aluminum-induced peptide aggregation process at the molecular level is an urgent scientific goal. A key issue is how the presence of Al(III) will influence the conformation of the peptide. Although the nuclear magnetic resonance (NMR) high-resolution A$\beta$P structure in nonaqueous medium is available (Zagorski & Barrow, 1992; Sticht *et al.*, 1995), structural models of the soluble monomeric adducts with aluminum or the insoluble oligomeric aluminated amyloids have not yet been determined.

Classic molecular dynamics (MD) simulations have proved to be a powerful tool to predict solution structures of peptide and proteins for which a high-resolution NMR or X-ray structure is lacking (see, e.g., Tirado–Rives & Jorgensen, 1990; Banci *et al.*, 1993; Banci *et al.*, 1994). Indeed, MD simulations have already been used to model the pH dependence of the conformation of the (1–28) residue A$\beta$P fragment (Kirshenbaum & Dagget, 1995). MD calculations also allow the mobility of residues in the biomolecule frame to be studied and are well suited for the analysis of adducts with small molecules and metal ions.

With the aim of determining the effect of Al binding on the conformation of the peptide, MD investigations of A$\beta$P and several models of its adducts with aluminum in aqueous solution at physiological pH have been undertaken. In addition, these calculations allow a detailed characterization of the structure of A$\beta$P in aqueous solution, which has hitherto been lacking.

# Computational Procedure

**Structural Models.** Our initial model is the 40-residue A$\beta$P in trifluoroethanol/water solution, whose high-resolution structure has been solved by NMR spectroscopy (Sticht *et al.*, 1995; first structure of the entry 1AML in the Protein Data Bank File, see Bernstein *et al.*, 1977).

To construct the A$\beta$P–Al adducts, we take into account that (i) at the low concentration of Al(III) in biological systems, polynuclear species are not important (Martin, 1986), (ii) Al(III) binds to proteins as aquaion ($Al^{3+}_{aq}$) in neutral aqueous solutions (Martin, 1986), and (iii) Al(III) preferentially binds to oxygen-based functional groups, especially to those belonging to carboxilate groups (Martin, 1986).

Inspection of the structure indicates that there are four highly probable metal sites (Fig. 1a): two (**I–II**) located at the N-terminus random coil and two (**III–IV**) closer to the central helix (His 14–Asp 23).[3] The aluminum coordination sites are shown in Fig. 1b. Water molecules complete the octahedral coordination polyhedra.

[3]The $\alpha$-helix content of the peptide is defined after Kabsch & Sander, 1983.

Because at physiological pH the overall charge of the peptide is $-3$, the A$\beta$P–Al adducts are neutral. To simulate the unbound A$\beta$P, we added three sodium ions close to Asp 1, Glu 3, and Asp 23. The systems were immersed in a water box having $3.6\times3.6\times4.8$-nm-long edges and a density of 1 g cm$^{-3}$. All the water molecules whose atoms were less than 0.25 nm from the solute were discarded. The resulting systems were composed of $\approx$6300 atoms.

**Parameterization.** The simulations were performed with the GROMOS96 program package (van Gunsteren *et al.*, 1996). The standard "united atom" GROMOS 43A1 force field was used for the biomolecule and the sodium ions. The water solvent was treated explicitly; to describe the water–water and water–biomolecule interactions we used a parameterization that is not present in the GROMOS 43A1 force field, namely the SPC model (Berendsen *et al.*, 1981). Analogously to the treatment of other nontransition-metal ions such as $Mg^{2+}$ and $Ca^{2+}$ (van Gunsteren *et al.*, 1996), we assume that the binding of $Al^{3+}$ is purely electrostatic in character (Martin, 1986); the Lennard–Jones parameters of Al(III) are those of the tetracoordinated Zn(II) ion (available in the package), the ionic radii of the two metal ions being quite similar (0.068 and 0.074 nm) (Cotton & Wilkinson, 1988).

**MD Calculations.** Periodic boundary conditions were applied. The nonbonded interactions were treated explicitly within a cutoff radius of 1.4 nm. Beyond this value, the electrostatic interactions were approximated using a Poisson–Boltzmann generalized reaction field (Tironi *et al.*, 1995). The time step of the dynamics was 1.5 fs. All bond lengths were kept constant using the SHAKE algorithm (van Gunsteren & Berendsen, 1977). The temperature was kept constant using the Berendsen thermostat (Berendsen *et al.*, 1984), with a relaxation time of 0.1 ps.

First, the water molecules were equilibrated by minimizing their rms energy gradient within 0.01 kJ mol$^{-1}$ and by performing MD simulations for 4.5 ps. Then a minimization was carried out on the entire system (rms energy gradient of less than 0.01 kJ mol$^{-1}$). The systems were heated gradually from 0 to 300 K by performing MD simulations for 15 ps at 100 K, 15 ps at 200 K, and 15 ps at 300 K. Finally, the MD simulations at 300 K were performed for a further 1.050 ns.

**Test Calculations.** To test the aluminum parameterization setup, we have carried out a MD simulation of $Al^{3+}$ in water. For this purpose, the metal ion was immersed in a water cubic box of 1.0 nm edge (water density 1 g cm$^{-3}$). The MD simulation was carried out at 300 K for 150 ps following the procedure outlined above. Analysis of the Al–O radial distribution function (Fig. 1, supplementary material) shows that the hydrated $Al^{3+}$ ion is a 6-coordinated one and that the Al–O distance is 0.190 nm, in very good agreement with experiment (Ohtaki & Radnai, 1993).

# Results

## Structure and Dynamics of A$\beta$P

In terms of root mean square displacement (rmsd), the structure of A$\beta$P equilibrates after 0.6 ns with respect to the initial model (the average rmsd for the heavy atoms during the final 0.495 ns being 0.6 nm). This indicates, as expected, a significant rearrangement of the structure on passing from fluoroethanol/water to water solutions.

Figure 2 indicates that on the nanosecond time scale, all A$\beta$P conformations have a significant contribution of $\alpha$-helical secondary structure. Whereas the long, central $\alpha$-helix is fairly well maintained from His 14 to Asp 23,[4] which is present in A$\beta$P in aqueous trifluoroethanol

[4]The $\alpha$-helix content of the peptide is defined after Kabsch & Sander, 1983.

solution (Sticht *et al.*, 1995), the Ile 31–Val 36 secondary structure is partially lost during the dynamics. The preservation of the central $\alpha$-helix is also evident when plotting snapshots of the backbone structure from the MD run (Fig. 3a). The Ramachandran plot (Ramachandran *et al.*, 1963) of the structure after 1.095 ns shows that the distribution of the $\psi$–$\phi$ angles is in the allowed region. In conclusion, MD calculations indicate that A$\beta$P is remarkably stable in aqueous solution, with considerable content of $\alpha$-helix structure.

### A$\beta$P–$Al^{3+}$ interactions

In binding to the peptide, $Al^{3+}$ does not perturb the peptide folding substantially.

The average rmsd values for the last 0.495 ps of the four aluminum adducts considered here are within the range 0.4–0.6 nm, and are thus quite similar to the unbound peptide values. In all adducts the central $\alpha$-helix is maintained during the dynamics. Figure 3, for instance, plots the $\alpha$-helical content of adduct **III** as a function of time. We see that in this case the Ile 31–Val 36 $\alpha$-helix is also maintained. The peptide structures, even though quite flexible, never rearrange and fold around the metal cation. Figure 3b shows, as an example, snapshots from the MD simulation of this adduct. Also for the aluminated peptides, the Ramchandran plots (Ramachandran *et al.*, 1963) of the structures after 1.095 ns show no $\psi$–$\phi$ pairs in disallowed regions.

The Al–O radial distribution functions, calculated for the last 0.495 ps, indicate that in all adducts, six oxygen atoms coordinate the metal ion. One or two donor atoms belong to the carboxylate groups of Gln or Asp residues of the peptide; the other ligands are water molecules. The backbone and side chain oxygens binding Al(III) in the starting adducts **I**–**IV** (Fig. 1b) are substituted by water molecules after a few tens ps of dynamics. Figure 3c, for instance, shows the structure of the Al(III) binding site of adduct **III** after 1.095 ns. We see that only one oxygen atom binding to Al(III) belongs to the peptide, namely the O$\epsilon$1 of Glu 11. Interestingly, the adduct is stabilized also by H bonds between three of the water molecules coordinated to the metal ion and the oxygen atoms of the peptide. These H-bond interactions are found in all the adducts studied here.

Energetically, the four adducts are very similar: their average potential energies differ by no more than 30 kJ $mol^{-1}$.

Our calculations suggest that the affinity of Al(III) for the four binding sites is quite similar both structurally and energetically.

## Discussion

A$\beta$P is poorly soluble; at relatively high concentrations it adopts an ensemble of different conformations and also oligomerizes. Therefore, MD calculations appear to be an attractive alternative approach to study the structure and dynamics of the peptide.

Here, our MD calculations provide the first detailed description of the structure and dynamics of the (1–40) residue A$\beta$P in water. The calculations indicate that on the nanosecond time scale the peptide is stable and does not unfold.

NMR studies have revealed the importance of the helical structure for the stabilization of the soluble form of A$\beta$P in nonaqueous solvent (Sticht *et al.*, 1995). The MD calculations suggest that, also in water, stabilization is due to the central $\alpha$-helix. However, a more recent NMR investigation in water (Lee *et al.*, 1995) yielded no evidence of a helical content of the peptide, and emphasized the importance of the (Ile 31–Met 35) and (Leu 17–Phe 20) hydrophobic regions for the stability of the peptide. In contrast to these findings, our calculations show that the hydrophobic side chains of these residues do not interact significantly during the dynamics, the distance between atoms of the different side chains being at least 0.5 nm.

The apparent discrepancy between experiment and theory can be rationalized if one considers that the relative predominance of a particular solution structure ($\alpha$-helix, $\beta$-sheet, or random coil) is strongly influenced by environmental factors, such as the peptide concentration and pH (Terzi *et al.*, 1995). Therefore, at the concentration required for NMR measurements, the peptide may have a very different conformation from that obtained with MD.

In conclusion, our calculations support the hypothesis that in water an equilibrium exists between the monomeric soluble form with high $\alpha$-helix and oligomers in which $\beta$-sheets prevail (Salomon *et al.*, 1996, and publications cited therein).

Upon Al binding, A$\beta$P rearranges itself from being partially helical to having a $\beta$-sheet conformation in trifluoroethanol/water (Exley *et al.*, 1993) and trifluoroethanol (Fasman *et al.*, 1995) solutions, and promotes its aggregation (Kawahara *et al.*, 1994). The mechanism of aggregation, however, is still unclear (Kawahara *et al.*, 1994). Our MD calculations indicate that aluminum binds to several structurally and energetically similar sites of the peptide without substantially affecting the structure of the peptide. Thus, the simulations suggest that aluminum is not a destabilizing factor *per se*. However, it can easily bind to Glu and Asp residues from different peptides and form cross links, in which O–Al–O oxo-bridges are present. The oligomeric aluminum adducts could then act as seeds for the amyloid fibrils and ultimately the plaques (Kawahara *et al.*, 1994).

# Acknowledgment

I thank W. Andreoni for useful discussions.

# References

[1] Banci, L., Bertini, I., Carloni, P., Capozzi, F., Ciurli, S., & Luchinat, C. (1993) *J. Am. Chem. Soc. 115*, 3431–3434.

[2] Banci, L., Carloni, P., & Savellini, G. G. (1994) *Biochemistry 33*, 12356–12366.

[3] Berendsen, H. J. C., Postma, J. P. M., van Gunsteren, W. F., & Hermans, J. (1981) in *Intermolecular Forces.* (Pullman, B., Ed.) pp 331–342, Reidel, Dordrecht.

[4] Berendsen, H. J. C., Postma, J. P. M., van Gunsteren, W. F., DiNola, A., & Haak, J.R. (1984) *Chem. Phys. 81*, 3684–3690.

[5] Bernstein, F. C., Koetzle, T. F., Williams, G. J. B., Meyer, E. F. Jr., Rodgers, J. R., Kennard, O., Shimanouchi, T., & Tasumi, M. (1977) *J. Mol. Biol. 112*, 535–542.

[6] Corain, B., Bombi, G. G., Tapparo, A., Perazzolo, M., & Zatta, P. (1996) *Coord. Chem. Rev. 149*, 11–22.

[7] Cotton, F. A. & Wilkinson, G. (1988) *Advanced Inorganic Chemistry*, 5th Ed., p 1387, Wiley, New York.

[8] Crapper, D. R., Krishnan, S. S., & Dalton, A. J. (1973) *Science 180*, 511–513.

[9] Exley, C., Price, N., Kelly, M. S., & Birchall, J. D. (1993) *FEBS Lett. 324*, 293–295.

[10] Fasman, G. D., Perczel, A., & Moore, C. D. (1995) *Proc. Nat'l Acad. Sci. USA 92*, 369–371.

[11] Good, P. F., & Perl, D. P. (1993) *Nature 362*, 418.

[12] Kabsch, W., & Sander, C. (1983) *Biopolymers 22*, 2577–2637.

[13] Kawahara, M., Muramoto, K., Kobayashi, K., Mori, H., & Kuroda, Y. (1994) *Biochem. Biophys. Res. Comm. 198*, 531–535.

[14] Kirshenbaum, K., & Dagget, V. (1995) *Biochemistry 34*, 7629–7639.

[15] Kraulis, Per J. (1991) *J. Appl. Cryst. 24*, 946–950.

[16] Landsberg, J. P., McDonald, B., & Watt, F. (1992) *Nature 360*, 65–68.

[17] Lee, J. P., Stimson, E. R, Ghilardi, J. R., Mantyh, P. W., Lu, Y.-A., Felix, A. M., Llamos, W., Behbin, A., Cummings, M., Van Criekinge, M., Timms, W., & Maggio, J. E. (1995) *Biochemistry 34*, 5191–5200.

[18] Martin, R. B. (1986) *Clin. Chem. 32*, 1797–1806.

[19] Newman, P. E. (1992) *Nature 360*, 65–68.

[20] Ohtaki, H., & Radnai, T., (1993) *Chem. Rev. 93*, 1157–1204.

[21] Perl, D. P., & Brody, A. R. (1980) *Science 208*, 297–299.

[22] Ramachandran, G. N., Ramakrishnan, C., & Sasisekharan, V. (1963) *J. Mol. Biol. 7*, 95–99.

[23] Salomon, A. R., Marcinowski, K. J., Friedland, R. P., & Zagorski, M. G. (1996) *Biochemistry 35*, 13568–13578.

[24] Selkoe, D. J. (1997) *Science 275*, 630–631, and references therein.

[25] Sticht, H., Bayer, P., Willbold, D., Dames, S., Hilbich, C., Beyreuther, K., Frank, R. W., & Roesch, P. (1995) *Eur. J. Biochem. 233*, 293–298.

[26] Terzi, E., Hölzemann, G., & Seelig, J. (1995) *J. Mol. Biol. 252*, 633–642.

[27] Tirado–Rives, J., & Jorgensen, W. L. (1990) *J. Am. Chem. Soc. 112*, 2773–2781.

[28] Tironi, I. G., Sperb, R., Smith, P. E., & van Gunsteren, W. F. (1995) *J. Chem. Phys. 102*, 5451–5459.

[29] van Gunsteren, W. F., & Berendsen, H. J. C. (1977) *Mol. Phys. 34*, 1311–1327.

[30] van Gunsteren, W. F., Billeter, S. R., Eising, A. A., Hünenberger, P. H., Krüger, P., Mark, A. E., Scott, W. R. P., & Tironi, I. G. (1996) *Biomolecular Simulation: the GROMOS96 Manual and User Guide*, Biomos, Zurich.

[31] Wisniewski, H. M., & Wen, G. Y. (1992) *Aluminum and Alzheimer Disease.* In *Aluminum in Biology and Medicine.* Ciba Foundation Symposium 169, pp 142–15, Wiley, Chichester.

[32] Zagorski, M. G., & Barrow, C. J. (1992) *Biochemistry 31*, 5621–5631.

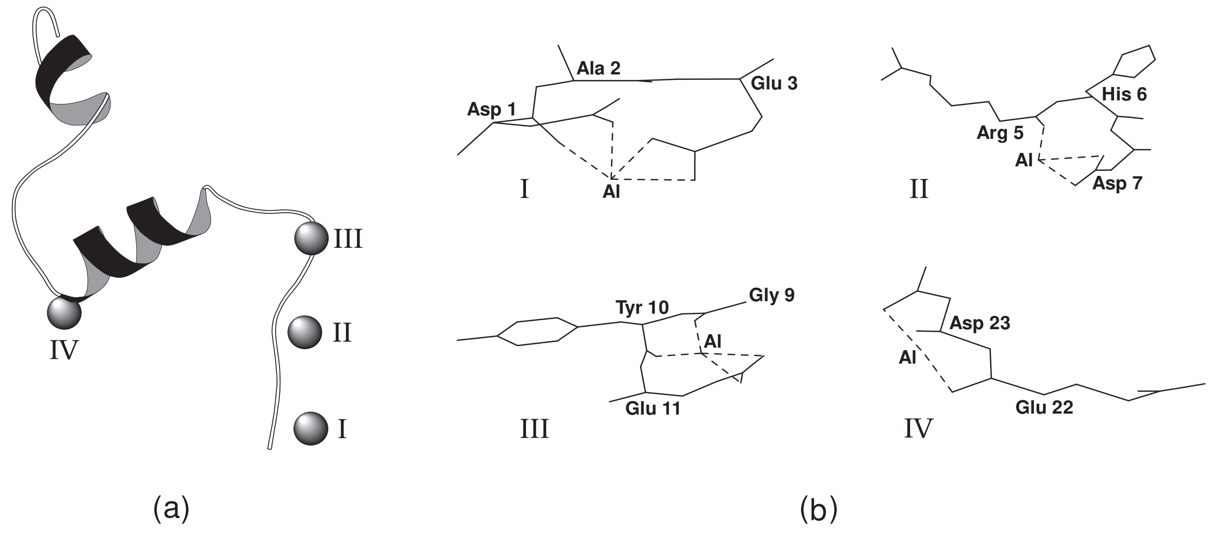


Figure 1: Four highly probable aluminum bindings sites in A$\beta$P: (a) backbone conformation and the aluminum ions are sketched (obtained using the Molscript program (Kraulis, 1991): (b) Local structure of the aluminum binding sites. In (a) the N–terminus is located at the bottom of the structure.

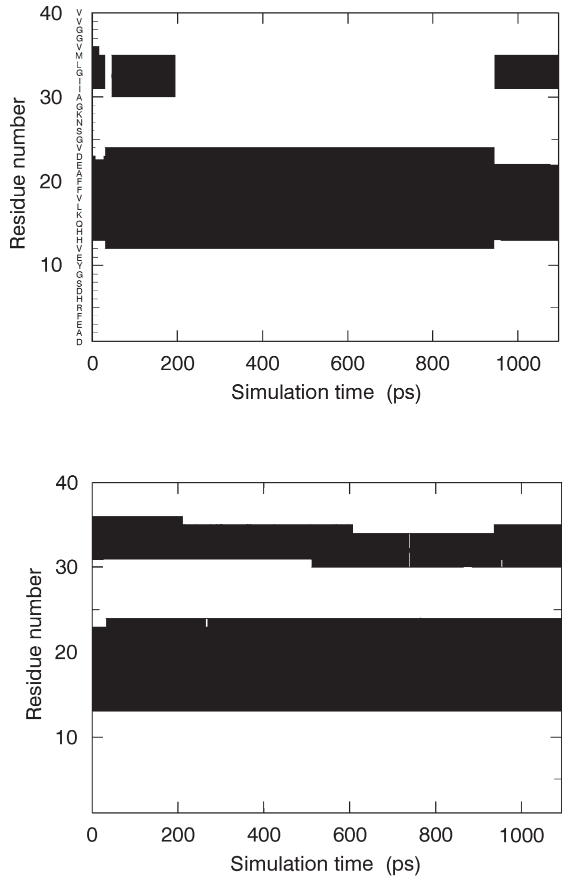


Figure 2: Helical content (defined after Kabsch & Sander, 1983) of A$\beta$P (top) and of its adduct **III** (bottom) plotted as a function of simulation time. The values are plotted every 0.3 ps.

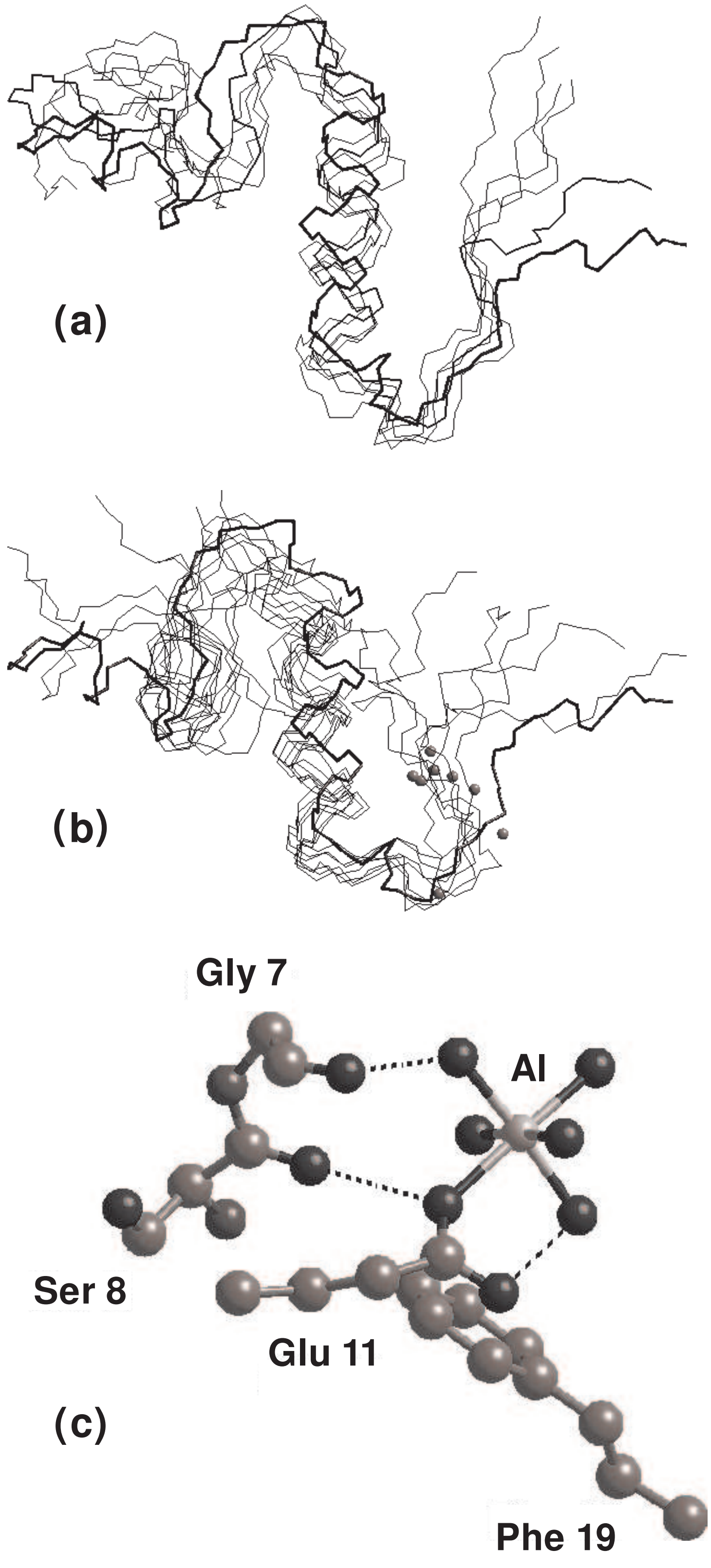


CAP36/ 0697

Figure 3: Dynamical models of (a) A$\beta$P and (b) its adduct **III**: The backbone structures are plotted at 0.0 (bold), 0.195, 0.345, 0.495, 0.645, 0.795, 0.945, and 1.095 ns. The $Al^{3+}$ ions are represented as spheres. (c) Aluminum binding sites of adduct **III** after 1.095 ns.

**Supplementary material.**
Figure 1: Al–O radial distribution function (thin) and its integral (thick), representing the coordination number of $Al^{3+}$.